Chinese Science Bulletin

The preparation and application of microbubble contrast agent combining ultrasound imaging and magnetic resonance imaging

YANG Fang, LI YiXin, CHEN ZhongPing & GU Ning †

State Key Laboratory of Bioelectronics, Jiangsu Laboratory for Biomaterials and Devices, School of Biological Science and Medical Engineering, Southeast University, Nanjing 210096, China

Encapsulated gas microbubbles are well known as ultrasound contrast agents (UCAs) for medical ultrasound (US) imaging. With the development of shell materials and preparation technologies, the application of microbubbles has been enormously popular in molecular imaging, drug delivery and targeted therapy, etc. The objective of this study is to develop Fe_3O_4 nanoparticle-inclusion microbubble construct. The *in vitro* US imaging experiment indicates that the Fe_3O_4 nanoparticle-inclusion microbubbles have higher US enhancement than those without Fe_3O_4 nanoparticle-inclusion. According to the microbubble dynamic theory, the acoustic scattering properties can be quantified by scattering cross-section of the shell. The scattering study on Fe_3O_4 nanoparticle-inclusion microbubbles of different concentration shows that within a certain range of concentration, the scattering cross-section of microbubble increases with the addition of Fe_3O_4 nanoparticles. When exceeding the concentration range, the ultrasonic characteristic of microbubbles is damped. On the other hand, since Fe_3O_4 nanoparticles can also serve as the Magnetic Resonance Imaging (MRI) contrast agent, they can be potentially used as contrast agents for the double-modality (MRI and US) clinical studies. However, it is important to control the concentration of Fe_3O_4 nanoparticles in the shell in order to realize the combined functions of US and MRI.

ultrasound (US) imaging, magnetic resonance imaging (MRI), microbubble, Fe_3O_4 nanoparticles, double-modality

Medical ultrasound is now a well-established technique for clinical diagnostics and will continue to play an important role in the foreseeable future. It is a noninvasive, real-time, portable, extremely safe method compared with X-ray and inexpensive relative to MRI[1]. However, ultrasound images do not have very sharp contrast and sometimes the area being imaged is buried and shadowed by tissues. This problem can be resolved in part by using ultrasound contrast agents (UCAs). UCAs are used to enhance the backscattered signal, and to improve resolution[2]. Microbubbles, commonly used as UCAs with the diameter of 1—10 μm, are prepared by several techniques, such as sonication, freeze drying, coaxial electrohydrodynamic atomization, high shear emulsification, and ink jet printing, etc.[3]. Under acoustic radiation, the scattered signal from the microbubble UCAs is much larger than that from the tissue[4]. The potential applications of microbubbles for imaging include tissue perfusion, inflammation, tumors, and in any tissue accessible to ultrasound interrogation, including liver, kidney, breast, spleen, and others[5–7]. New objectives include agents that target specific cells for molecular imaging[8–10], and drug and gene delivery[11–13].

In general, a shell encapsulating the gas bubble is essential for the longevity of the microbubble. The shell may be composed of surfactant[14], protein[15], lipid[16,17]

Received November 6, 2008; accepted February 4, 2009
doi: 10.1007/s11434-009-0168-5
†Corresponding author (email: guning@seu.edu.cn)
Supported by the National Basic Research Program of China (Grant No. 2006CB933206) and National Natural Science Foundation of China (Grant No. 50872021)

Citation: Yang F, Li Y X, Chen Z P, et al. The preparation and application of microbubble contrast agent combining ultrasound imaging and magnetic resonance imaging. Chinese Sci Bull, 2009, 54: 2934—2939, doi: 10.1007/s11434-009-0168-5

or polymer materials[18,19]. The novel UCAs is also emerging, such as micro- or nano-emulsion, silicon oxide nanoparticles[20], gold nanoparticles[21], and other nanoparticles[22,23]. Nowadays, the wide variety of both synthetic and natural polymers-based products has encouraged their use with biotechnological applications to drug delivery systems, tissue engineering, regeneration medicine, and more recently, to imaging. Polymer shell-based microbubbles have many advantages. They are more stable under ultrasonic waves than monomolecular layers of proteins, lipids, or surfactants because they have better mechanical strength. The elasticity of the shells can be controlled by adjusting the chemical composition and the molecular weight of the polymer[24]. Also, the shell provides a good surface for conjugating with target-specific ligands and for the drug loaded. When combined with specific targeted imaging and drug delivery, polymer shell-based agents can realize the functions of diagnosis, therapy, etc[25].

Among all medical imaging modalities, no single modality is perfect and sufficient to obtain all the necessary information. For example, MRI has high resolution yet it suffers from low sensitivity. Radionuclide- based imaging techniques have very high sensitivity but they have relatively poor resolution. Although microbubbles can improve the accuracy and confidence of disease diagnosis by providing higher quality images and can play a decisive role in clinical decision making, ultrasound has some disadvantages such as relatively limited sensitivity. Therefore the combination of US and other imaging modalities can offer synergistic advantages over any modality alone[26,27].

In this study, the Fe_3O_4 nanoparticles were encapsulated in the shell of microbubbles, which can be used as potential US and MRI double imaging modality contrast agents. By optimizing the concentration of Fe_3O_4 nanoparticles in the shell, the multimodality contrast agents combining the advantages of the US and MR imaging can be applied clinically. Thus adequate and comprehensive imaging information can be obtained by using one multifunctional contrast agent.

1 Materials and methods

1.1 Preparation of microbubbles

Poly (D, L-lactide) (10000 W), PLA, was purchased from Shandong Key Laboratory of Medical Polymer Materials. Poly (vinyl alcohol) (PVA), 89mol% hydrolyzed with a MW of 25000 was from Alfa Aesar®. Fe_3O_4 nanoparticles with mean diameter of 12 nm were prepared by Chen Zhongping etc[28]. Other agents were of the analytical grade.

PLA (0.5 g) was dissolved in 10 mL of methylene chloride. To generate the first W/O emulsion, 1.0 mL of de-ionized water was added to the polymer solution and probe sonicated at 200 W while constant purging using a steady (4 mL/min) stream of N_2 gas for 2 min. The W/O emulsion was then poured into a 5% PVA solution and homogenized for 2 h at 3000 $r \cdot min^{-1}$ by mechanical stirring. The microbubbles were then collected by centrifugation (at 15℃ for 5 min at 1500 $r \cdot min^{-1}$), washed three times with de-ionized water, and collected the samples.

1.2 Characterization of microbubbles

The mean diameter size and size distribution of the microbubbles were analyzed using a Laser Diffraction Particle Size Analyzer (Mastersizer 2000, England). Milli-Q pure water was used as the blank solution, and the sample was added until an appropriate concentration was indicated. Each sample was tested in triplicate.

Samples in solution were placed between glass slides and observed with an Axioskop 40 microscope equipped with a Coolsnap MP3.3 camera (Carl Zeiss, Germany).

In order to verify whether or not the nanoparticles were encapsulated into the shell, their morphology and structure were determined by transmission electron microscopy (TEM). The concentration of Fe_3O_4 nanoparticles embedded in the shell of microbubbles was determined by an AA240FS Atomic Absorption Spectrometer (Hitachi, Japan).

1.3 *In vitro* US imaging of microbubbles

In vitro ultrasound imaging experiment was performed by exposing a sample by the self-made acoustic setup. An anechoic water tank, 12 cm long, 6 cm wide, 6.5 cm deep, was used and 2 cm thick sponge layer was placed to the bottom as the acoustic absorber. The solution was contained in a silica gel tube (diameter ϕ4×6 mm) and then the tube was sealed and fixed in the water tank 4 cm from the bottom of the tank. Each tube was filled with either de-ionized water, or Fe_3O_4-inclusion microbubbles, or microbubbles without Fe_3O_4 nanoparticles. There should be no air in the tube. The B-mode ultrasound image of the sample was acquired using a 3.5 MHz centre frequency transducer of the ultrasonic im-

aging system provided by Belson Imaging Technology Co., Ltd. (Wuxi, China), and stored on the internal hard drive for off-line processing. All the samples were scanned using the above method and the settings of system were kept unchanged during the scan of all the samples (dynamic range 0—70 dB, edge enhancement 4 and receiver gain 50 dB). To quantitatively measure image brightness, a mean grey scale was calculated as the average of the grey scale levels of all pixels within a region of interest (ROI) by using a MatLab computer program.

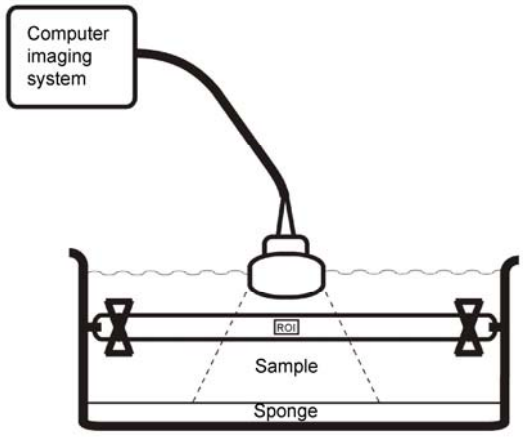

Figure 1 The schematic diagram of *in vitro* US imaging.

1.4 Microbubble dynamic experiment in the ultrasound field

The dynamics behavior of microbubble is the basis for the explanation, understanding and prediction of the contrast efficiency. According to the microbubble dynamic theory, the scattering can be quantified by scattering cross-section, which is relative to the excitation frequency, the size of the bubble and the viscoelastic properties of the shell[29]. The Fe_3O_4 nanoparticle embedded shell is a new structure which may bring the microbubble new scattering property. In order to study the relationship between the concentration of the nanoparticles and the scattering cross-section, the Hoff model[30] is used to calculate the scattering cross-sections of the samples with different concentration of Fe_3O_4 nanoparticle inclusion.

Based on the acoustic attenuation measurement, the elasticity parameter G_s and viscosity parameter μ_s of the shell were estimated by using an optimization method. Then with the estimated parameter values, the scattering cross-section of each sample was calculated given the excitation frequency as 3.5 MHz and the microbubble radius as 2 μm.

1.5 *In vitro* MRI experiment

The de-ionized water and different Fe_3O_4 nanoparticle-inclusion microbubbles were put into the 1 mL Eppendorf tubes. MRI of these tubes was performed with a clinical 1.5T MR imager (Eclipse, Philips Medical Systems, the Netherlands) by using a 12.7 cm long receive-only surface coil. The MRI sequence was a T_2 (spin-spin interaction time constant)-weighted fast spin-echo (4000/108; echo train length, 16) sequence. Images were obtained with a matrix size of 254×254, section thickness of 2 mm and field of view of 12 cm×12 cm. Three measurements were acquired for each sample separately. The transverse relaxation rate (R_2) as a function of the Fe_3O_4 nanoparticle concentration was then calculated based on the measured T_2 data.

2 Results and discussion

2.1 Characterization of microbubbles

The average mean diameter size (each sample for triplicate) was found to be about 3.98 μm with polydispersity index (PI) of 1.13 and the experimental microbubble concentration was diluted at $5—6\times10^6$ microbubbles/mL. The measured encapsulated Fe_3O_4 nanoparticle concentration in the shell were 0, 47.80, 86.47, 124.99, 191.46 μg/mL respectively.

The morphology was observed under the light microscopy (Figure 2). The microbubbles are spherical. There are no significant difference between Fe_3O_4 nanoparticle-inclusion microbubbles and microbubbles without Fe_3O_4 nanoparticles.

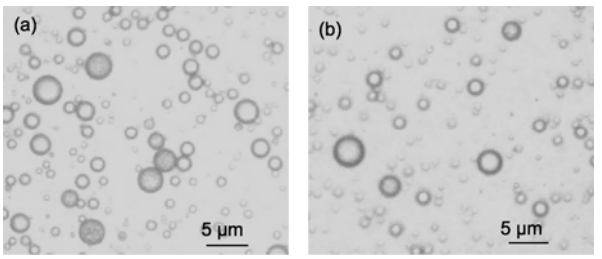

Figure 2 Microscopic images of microbubbles. (a) Microbubbles without Fe_3O_4 nanoparticles; (b) Fe_3O_4 nanoparticle-inclusion (47.80 μg/mL) microbubbles.

The TEM morphology of microbubbles is shown in Figure 3. The results show that the Fe_3O_4 nanoparticles are dispersed uniformly in the polymer layer. It is found that the addition of nanoparticles in the shell do not sig-

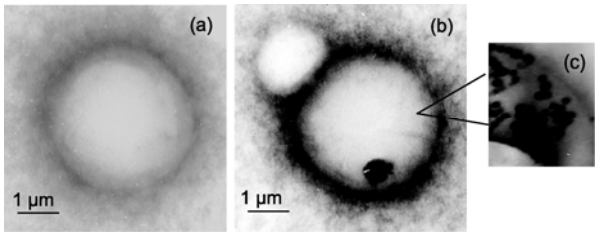

Figure 3 TEM images of microbubbles. (a) Microbubbles without Fe_3O_4 nanoparticles; (b) Fe_3O_4 nanoparticle-inclusion (47.80 μg/mL) microbubbles; (c) the enlarged TEM view of the local shell layer corresponding to image (b).

nificantly influence the thickness of shell.

There is also no obvious change observed in morphology, size and size distribution after 2-week storage.

2.2 *In vitro* ultrasound imaging experiment

The ultrasound images of the de-gassed and de-ionized water, the microbubbles without Fe_3O_4 nanoparticle-inclusion and the Fe_3O_4 nanoparticle-inclusion microbubbles (47.80 μg/mL) were captured. They are respectively shown in Figure 4(a)—(c). Compared with the de-gassed and de-ionized water, the brighter area can be seen distinctly in the microbubbles without Fe_3O_4 nanoparticle-inclusion and the Fe_3O_4 nanoparticle-inclusion microbubbles. The results also show that the image of Fe_3O_4 nanoparticle-inclusion microbubbles (Figure 4(c)) is brighter than that of the microbubbles without Fe_3O_4 nanoparticles (Figure 4(b)). It suggests that the inclusion Fe_3O_4 nanoparticles in the shell also contribute to ultrasound back-scattering echo intensity.

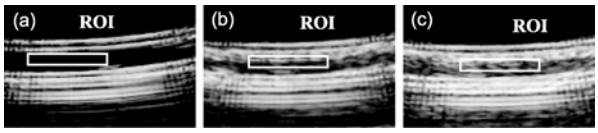

Figure 4 The *in vitro* ultrasound imaging in the different samples. (a) De-gassed and de-ionized water; (b) the microbubbles without Fe_3O_4 nanoparticles; (c) the Fe_3O_4 nanoparticle-inclusion microbubbles.

The mean grey scales within the ROIs of Figure 4(a)—(c) are shown in Table 1. It indicates that at the same microbubble concentration, Fe_3O_4-inclusion microbubbles have 12.3 greater mean grey scale enhancement than microbubbles without Fe_3O_4. It can be inferred that the Fe_3O_4 nanoparticles in the shell also have contributions to the ultrasound imaging enhancement.

Table 1 The mean grey scale within ROI corresponding to US images

Type of microbubble	Mean grey scale
De-gassed and de-ionized	15.8
Microbubbles without Fe_3O_4 nanoparticles	72
Fe_3O_4 nanoparticle-inclusion microbubbles	84.3

2.3 US enhancement mechanism of different Fe_3O_4 nanoparticle-inclusion concentration microbubbles

From Table 2, it is found that, with the increase of Fe_3O_4 nanoparticle-inclusion concentration in the shell of microbubbles, the viscoelastic parameters of shells decrease at first and then increase. The corresponding changes of scattering cross-section have the contrary tendency when under 3.5 MHz excitation frequency and with 2 μm radius. With the increasing concentration of Fe_3O_4 nanoparticles in the shell, the scattering cross-sections increase at first and then decrease. It can be inferred that the mechanism of the enhancement of the contrast efficiency is that the nanoparticles inclusion can change the viscoelastic properties of the shell. With the increase of the inclusion concentration, the echogenic enhancement is increased till the insertion concentration reaches about 86.47 μg/mL. When the inclusion concentration exceeds 86.47 μg/mL, the Fe_3O_4 nanoparticles make the shell become stiffer and can damp the ultrasonic character of microbubbles. Therefore, by depositing appropriate solid nanoparticles on the surface of microbubbles, the echo character of the microbubble response can be changed significantly.

2.4 *In vitro* MRI experiment

The MRI experiment in Figure 5 indicates that the more Fe_3O_4 nanoparticles were encapsulated in the shell, the darker MR image in the Eppendorf tube can be observed.

Table 2 The viscoelastic parameter values of the studied samples

Fe_3O_4-inclusion concentration (μg/mL)	Elasticity parameter G_s (MPa)	Viscosity parameter μ_s (Pa)	Scattering cross-section (μm^2)
0	1.70E+01	1.87E-01	265.5976
47.80	1.25E+01	1.58E-01	594.8477
86.47	1.34E+01	1.51E-01	608.8628
124.99	1.31E+01	1.63E-01	557.2473
191.46	1.85E+01	2.02E-01	189.5453

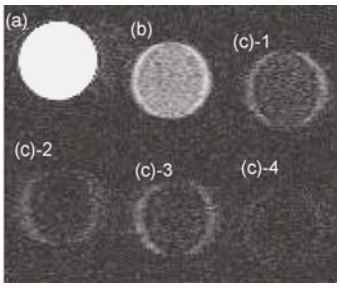

Figure 5 The *in vitro* ultrasound imaging in the different samples. (a) De-gassed and de-ionized water; (b) the microbubbles without Fe_3O_4 nanoparticles; (c) Fe_3O_4 nanoparticle-inclusion microbubbles at differeat concentration: c-1, 47.80, c-2, 86.47, c-3, 124.99, c-4, 191.46 μg/mL.

That is to say, MRI is much better with the increase of the Fe_3O_4 nanoparticle-inclusion concentration.

Figure 6 shows the function relationship of R_2 and the concentration of Fe_3O_4 nanoparticles in the shell. The data fitted to a linear function with the correlation coefficient r = 0.9606. It seems to suggest that with the increase of Fe_3O_4 nanoparticle in the shell, the transverse relaxation rate R_2 of microbubbles is bound to increase.

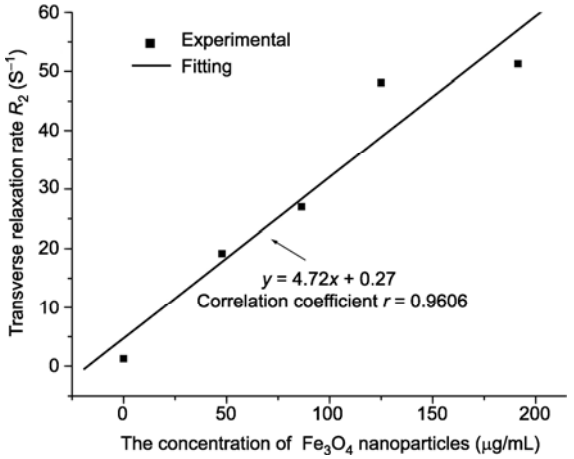

Figure 6 The linear fit was obtained between the Fe_3O_4 nanoparticle-inclusion concentration in the microbubbles and the transverse relaxation rate (R_2).

2.5 Optimization of Fe_3O_4-inclusion concentration in the shell of microbubbles

The Fe_3O_4-inclusion concentration in the shell of microbubble should be deliberately designed. The US imaging experiment and shell dynamic study indicate that, within a certain concentration range, the insertion of nanoparticles in the shell can not influence the viscoelasticity to contract and expand in response to the ultrasound wave, which makes the microbubbles have better acoustic back-scatter response. Once exceeding certain concentration range, the shell becomes stiffer and impedes the ability of the microbubbles to resonate. However, on the other hand, the *in vitro* MRI experiments show that more Fe_3O_4 nanoparticles result in better MRI effect. Therefore, in order to fabricate the dual contrast agents for US and MRI, it is very important to control the nanoparticle concentration in the shell. In our study, the optimized Fe_3O_4 nanoparticle concentration is 86.47 μg/mL. Such Fe_3O_4-inclusion microbubbles can be potential used as US and MRI multimodality contrast agents.

3 Conclusions

Microbubble contrast agents have created new opportunities for ultrasound. In this study, Fe_3O_4 nanoparticles of 12 nm were successfully encapsulated in the polymer shell of microbubbles. The *in vitro* US and acoustic attenuation experiments have shown that it is possible that the effective echogenic characteristics of microbubbles can be significantly enhanced through the optimization of the embedding nanoparticles in the shell. The *in vitro* MRI experiment shows that microbubbles with Fe_3O_4 nanoparticles can also be useful MRI contrast agents. On the other hand, the microbubbles should be acoustically responsive. Therefore, when appropriate Fe_3O_4 nanoparticles are fabricated into the shell to satisfy the above criteria, such microbubbles can potentially be used as contrast agents for double- modality (MRI and US) clinical studies. Our work is preliminary although encouraging, and further *in vitro* and *in vivo* studies are necessary before they can be used as new contrast agents.

1 Schutt E G, Klein D H, Mattrey R M, et al. Injectable microbubbles as contrast agents for diagnostic ultrasound imaging: The key role of perfluorochemicals. Angew Chem Int Ed, 2003, 42: 3218－3235
2 Lencioni R. Impact of European Federation of Societies for Ultrasound in Medicine and Biology (EFSUMB) guidelines on the use of contrast agents in liver ultrasound. Eur Radiol, 2006, 16: 1610－1613
3 Stride E, Edirisinghe M. Novel microbubble preparation technologies. Soft Matter, 2008, 4: 2350－2359
4 Correas J M, Bridal L, Lesavre A, et al. Ultrasound contrast agents: Properties, principles of action, tolerance, and artifacts. Eur Radiol, 2001, 11: 1316－1328
5 Cosgrove D. Ultrasound contrast agents: An overview. Eur J Radiol, 2006, 60: 324－330
6 Leen E, Moug S J, Horgan P. Potential impact and utilization of ul-

trasound contrast media. Eur Radiol, 2004, 14(suppl 8): 16－24
7 Miller D L, Averkiou M A, Brayman A A, et al. Bioeffects considerations for diagnostic ultrasound contrast agents. J Ultras Med, 2008, 27: 611－632
8 Cavalieri F, Hamassi A E, Chiessi E, et al. Tethering functional ligands onto shell of ultrasound active polymeric microbubbles. Biomacromolecules, 2006, 7: 604－611
9 Dayton P A, Pearson D, Clark J, et al. Ultrasonic analysis of peptide- and antibody-targeted microbubble contrast agents for molecular imaging of $\alpha_v\beta_3$- expressing cells. Mol Imaging, 2004, 3: 125－134
10 Alexander L K. Ligand- carrying gas- filled microbubbles: Ultrasound contrast agents for targeted molecular imaging. Bioconjugate Chem, 2005, 16: 9－17
11 Liu Y, Miyoshi H, Nakamura M. Encapsulated ultrasound microbubbles: Therapeutic application in drug/ gene delivery. J Control Release, 2006, 114: 89－99
12 Ng K, Liu Y. Therapeutic ultrasound: Its application in drug delivery. Med Res Rev, 2002, 22: 204－223
13 Lentacker B I, Smedt S C D, Demeester J, et al. Lipoplex-loaded microbubbles for gene delivery: A trojan horse controlled by ultrasound. Adv Funct Mater, 2007, 17: 1910－1916
14 Brian E O, Margaret A W. Development and characterization of a nano-scale contrast agent. Ultrasonics, 2004, 42: 343－347
15 Maayan D E, Dan A, Marcelle M. The effects of albumin-coated microbubbles in DNA delivery mediated by therapeutic ultrasound. J Control Release, 2006, 112: 156－166
16 Arnaud B, Patrick S, Francois H, et al. Design of targeted lipid nanocapsules by conjugation of whole antibodies and antibody Fab'fragments. Biomaterials, 2007, 28: 4978－4990
17 Unger E C, Porter T, Culp W, et al. Therapeutic application of lipid-coated microbubbles. Adv Drug Deliver Rev, 2004, 56: 1291－1314
18 Pisani E, Tsapis N, Paris J, et al. Polymeric nano/ microcapsules of liquid perfluorocarbons for ultrasonic imaging: Physical characterization. Langmuir, 2006, 22: 4397－4402
19 Kim J H, Park K, Nam H Y, et al. Polymers for bioimaging. Prog Polym Sci, 2007, 32: 1031－1053
20 Liu J, Levine A L, Mattoon J S, et al. Nanoparticles as imaging enhancing agents for ultrasonography. Phys Med Biol, 2006, 51: 2179－2189
21 Bekeredjian R, Behrens S, Ruef J, et al. Potential of gold-bound microtubules as a new ultrasound contrast agent. Ultrasound Med Biol, 2002, 28: 691－695
22 Ingo N, Giles H V, Mathias M, et al. Iron particles enhance visualization of experimental gliomas with high-resolution sonography. Am J Neuroradiol, 2005, 26: 1469－1474
23 Oh J, Feldman M D, Kim J, et al. Detection of magnetic nanoparticles in tissue using magneto-motive ultrasound. Nanotechnology, 2006, 17: 4183－4190
24 Cavalieri F, Finelli I, Tortora M, et al. Polymer Microbubbles as diagnostic and therapeutic gas delivery device. Chem Mater, 2008, 2010): 3254－3258
25 Cavalieri F, Hamassi A E, Chiessi E, et al. Stable polymeric microballoons as multifunctional device for biomedical uses: synthesis and characterization. Langmuir, 2005, 21: 8758－8764
26 Townsend D W. Multimodality imaging of structure and function. Phys Med Biol, 2008, 53: R1－R39
27 Cai W, Chen X. Nanoplatforms for targeted molecular imaging in living subjects. Small, 2008, 3: 1840－1854
28 Chen Z P, Zhang Y, Zhang S, et al. Preparation and characterization of water-soluble monodisperse magnetic iron oxide nanoparticles via surface double-exchange with DMSA. Colloid Surface A, 2008, 316: 210－216
29 Church C C. The effects of an elastic solid surface layer on the radial pulsations of gas bubbles. J Acoust Soc Am, 1995, 97: 1510－ 1521
30 Hoff L, Sontum P C，Hovem J M. Oscillations of polymeric microbubbles: Effect of the encapsulating shell. J Acoust Soc Am, 2000, 107: 2272－2280